

**STUDY OF STRUCTURAL AND ELECTRICAL TRANSPORT
PROPERTY OF YBCO+ BaTiO₃-CoFe₂O₄
SUPERCONDUCTOR**

A REPORT SUBMITTED
TO
DEPARTMENT OF PHYSICS
NATIONAL INSTITUTE OF TECHNOLOGY, ROURKELA



BY
Bishnupriya Bhol
M.Sc Physics
Roll No. - 410PH2120

Under the supervision of
Prof. D. Behera
Department of Physics, NIT Rourkela



**NATIONAL INSTITUTE OF TECHNOLOGY
ROURKELA**

CERTIFICATE

This is to certify that the thesis entitled “**Study of Structural and Electrical Transport Property of YBCO+ BaTiO₃-CoFe₂O₄ Superconductor**” submitted by Miss. Bishnupriya Bhol in partial fulfilments for the requirements for the award of Master of Science Degree in Physics Department at National Institute of Technology, Rourkela is an authentic work carried out by him under my supervision and guidance.

To the best of my knowledge, the matter embodied in the project has not been submitted to any other University/ Institute for the award of any Degree or Diploma.

(D. Behera)

ACKNOWLEDGEMENT

With deep regards and profound respect, I avail this opportunity to express my deep sense of gratitude and indebtedness to my guide Prof. D.Behera of Department of Physics, National Institute of Technology Rourkela, for introducing the present project topic and for his inspiring guidance, constructive criticism and valuable suggestion throughout the project work. I most gratefully acknowledge his constant encouragement and help in different ways to complete this project successfully.

I would like to acknowledge my deep sense of gratitude to Prof.S. Jena, Head of Department of Physics, National Institute of Technology, Rourkela for his valuable advices and constant encouragement for allowing me to use the facilities in the laboratory.

It give me great pleasure to express my heartfull gratitude to the laboratory mates Ms. Mousmibala Shaoo, Ms. Arpna Kujur and Mr. Ranjit Panda for sharing their ideas with me and taking part in my project work by providing me a friendly humorous and amicable atmosphere to work .

I wish to thank all the faculty members & staff of Department of Physics for their support and help during the project. Last but not the least, I would like to express my gratefulness to my parents for their endless support, without which I could not complete my project work. I would also like to thanks to my friends and all the Ph.D students in our physics department for their valuable help.

Rourkela

Date:

Bishnupriya Bhol

DECLARATION OF THE CANDIDATE

I here by declare that the project work entitled “**Study of Structural and Electrical Transport Property of YBCO+ BaTiO₃-CoFe₂O₄ Superconductor**” is an authentic work carried by me, during the one year project at NIT, Rourkela, from July 2011 to May 2012 under the supervision of Dr. Dhruvananda Behera and is being submitted for the partial fulfillment of the requirement for award of the degree of Master of Science in Physics to NIT, Rourkela. This has not been submitted anywhere else for the award of any other degree.

Date

Bishnupriya Bhol

ABSTRACT

Pristine $\text{YBa}_2\text{Cu}_3\text{O}_{7-\delta}$ (YBCO) and Magnetolectric composite $\text{BaTiO}_3\text{-CoFe}_2\text{O}_4$ (BTO-CFO) samples are prepared by solid state route. Magnetolectric (ME) materials are used as composite because of its advantageous properties. These materials are promising candidates for technological applications, since the multiferroic coupling allows the interconnection between magnetic and electric fields. New memory devices electrically written and magnetically read have been proposed that are based on ME materials. $\text{BaTiO}_3\text{-CoFe}_2\text{O}_4$ composites are interesting magnetolectric materials due to the individual properties of their components. CoFe_2O_4 has a spinel structure with large coercivity and magnetostriction. The tetragonal BaTiO_3 is the most interesting due to its ferroelectric and piezoelectric properties.

XRD shows that all samples have orthorhombic phase at room temperature with a space group P_{mmm} without noticeable impurity peaks. The Resistivity vs. Temperature was done by four probe method. It is found that by increasing the wt.% of BTO-CFO in the YBCO matrix the transition temperature (T_C) decreases gradually.

CONTENTS

Chapter I

Introduction

- 1.1 General Remarks
- 1.2 Types of superconductor
- 2.1 $\text{YBa}_2\text{Cu}_3\text{O}_{7-x}$ High Tc Superconductor
- 2.2 Magnetoelectric Material
- 2.3 BaTiO_3 - CoFe_2O_4 Magnetoelectric System

Chapter II

Experimental Procedure

- 3.1 Preparation of YBCO
- 3.2 Preparation of CoFe_2O_4
- 3.3 Preparation of BaTiO_3
- 3.4 Preparation of BaTiO_3 - CoFe_2O_4 Composite

Chapter III

Characterization

- XRD Analysis
- R-T Measurement by Four probe method

Chapter IV Results and Discussion

Chapter V Conclusion

REFERENCES

Chapter I

1. INTRODUCTION

1.1 General remarks :

Superconductivity is the property of a material. Some materials show this property when they are cooled to a temperature below the room temperature. What is this property? As the name superconductivity suggests, the conductivity of the material is very high and resistance is very low, approaches to zero. As one cools, the material below a certain temperature the resistance becomes zero. This temperature is termed as superconducting transition temperature or critical temperature T_c . Below a temperature (i.e. T_c) the material is said to attend a zero resistance state called superconducting state. Dutch Physicist H. Kamerlingh Onnes first discovered the phenomenon of superconductivity in Mercury in 1911 nearly 100 years ago from year, 2011. The magnetic behaviour shows perfect diamagnetic at superconducting state. As resistance is zero it is devoid of Joules heating. The conductivity is infinity with no loss of energy. A dramatic change in the research activity has taken place when high temperature superconductors (HTSC) having T_c of 90 K, above the boiling point of liquid nitrogen (77 K), was discovered in $\text{YBa}_2\text{Cu}_3\text{O}_{7-\delta}$ (YBCO) in the year 1986. The operating device with zero-resistance at liquid-nitrogen temperature has fuelled world wide interest for power applications like superconducting magnets, motors and power-transmission lines etc. Superconducting magnets are used for nuclear fusion experiments (LHC), superconducting magnetic resonance imaging (MRI), magnetically levitated train (Maglev) and in other future commercial transportation systems. In the field of electronics, extensive studies on Josephson junction, Josephson computers and the development of commercial superconducting quantum interference device (SQUID) systems are now applied for characterization of materials.

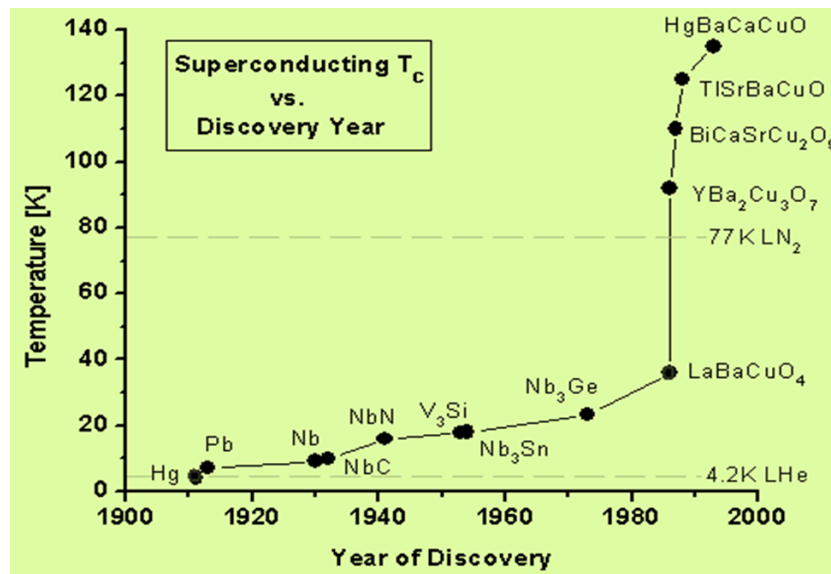


Fig.1 Chronological development of superconductors

Depending on their response to magnetic properties superconductors are classified into two types :

- (1) Type-I superconductor
- (2) Type-II superconductor

Type-I superconductor : All the elemental superconductors exhibit flux expulsion (Meissner effect) up to a critical magnetic field (H_C) beyond which flux penetrates the material and drives it to normal state. This type of superconductors is called of type-I superconductor. Very pure samples of Pb, Hg and Sn are examples of Type-I superconductors. Type-I superconductors are also known as soft superconductors as they can not bear high magnetic field. With small field they are turned to normal materials.

Type-II superconductors : Type-II superconductors are also known as hard superconductors due to bearing of high magnetic field. High temperature ceramic cuprate superconductors such as YBCO, BSCCO, TlBCCO, HBCCO are the examples of Type II superconductors. This type of superconductivity is exhibited by transition metals with high values of the electrical resistivity in the normal state i.e. the electronic mean free path in the normal state is short.

The figure below shows the behavior of magnetic field to material. It obeys Meissner effect upto certain critical field H_{c1} at which magnetic flux begins to enter the superconductor and an upper critical field H_{c2} at which superconductivity disappears.

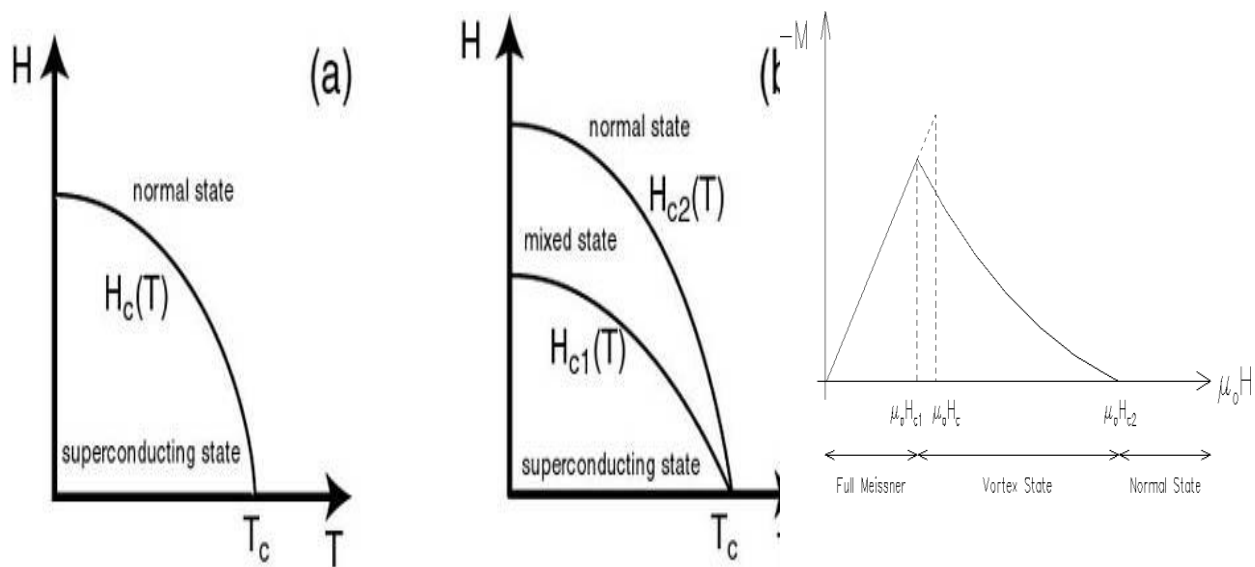


Fig.2: Magnetic phase diagram $H(T)$ for (a) Type-I superconductors : one critical field H_c exists (b) Type-II superconductors : where two critical fields exist (Lower critical field (H_{c1}) & upper critical field (H_{c2})).

2. High - T_c Superconductor

Depending on transition temperature superconductors are also classified as low T_c and high T_c superconductors. Low T_c superconductors are basically BCS superconductors. The superconductors above 30 K are high T_c superconductors. The transition temperature obtained in the materials crosses the limit of BCS prediction. Hence, named as high temperature superconductor (HTSC). These materials are type II superconductors having large vortex state useful for large magnetic field applications.

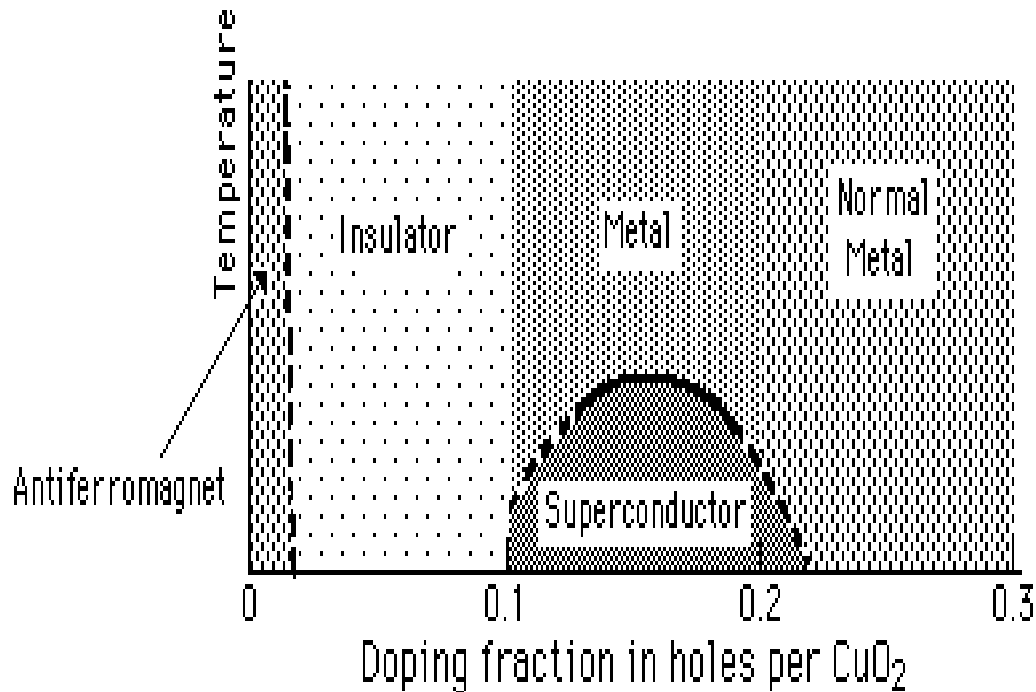


Fig.3 Phase diagram of cuprate superconductor

Phase diagram of cuprate materials shows long range order of an antiferromagnet at very low doping. With increasing the Doping level antiferromagnetic order breaks and they become insulators. Only with doping fraction between about 0.1 and 0.2 do they become superconductors.

2.1 YBa₂Cu₃O_{7-x} : Yttrium Barium Copper Oxide, often abbreviated as YBCO, is a crystalline chemical compound with the formula YBa₂Cu₃O₇. This material is a famous high-temperature superconductor, because it was the first material to achieve superconductivity above the boiling point of liquid nitrogen i.e 77 K. The proportions of the 3 different metals in the YBa₂Cu₃O₇ superconductor are in the mole ratio of 1:2:3 Yttrium to barium to copper respectively. So this superconductor is often referred to as the 123 superconductor. The structure of a high T_c superconductor is closely related to perovskite structure, and the structure of these compound has been described as a distorted, oxygen deficient multi-

layered perovskite structure. One of the properties of the crystal structure of oxide superconductor is an alternating multilayer of CuO_2 planes with superconductivity taking place between these layers. The more the layers of CuO_2 , the higher the T_c .

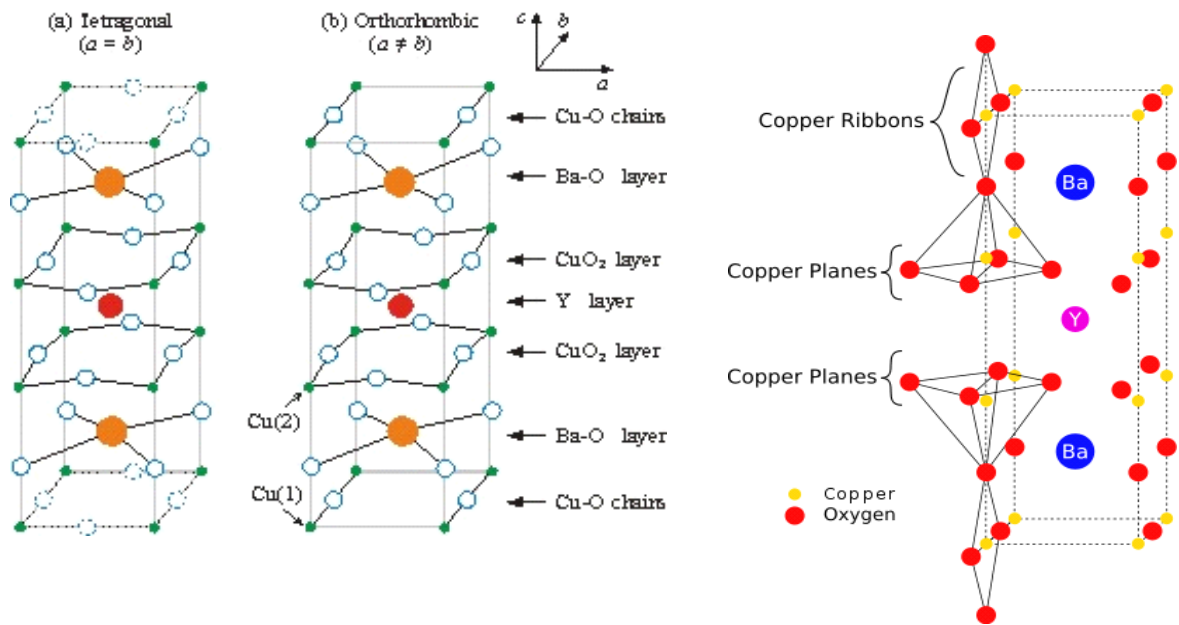


Fig.4. Unit cell of YBCO having tetragonal and Orthombic structure.

The unit cell of $\text{YBa}_2\text{Cu}_3\text{O}_7$ consists of three pseudocubic elementary perovskite unit cells. Each perovskite unit cell contains a Y or Ba atom at the centre, Ba in the bottom unit cell, Y in the middle one, and Ba in the top unit cell. Thus, Y and Ba are stacked in the sequence Ba-Y-Ba along the c-axis. YBCO crystallises in a defect perovskite structure consisting of layers. The boundary of each layer is defined by planes of square planar CuO_4 units sharing 4 vertices. The planes can sometimes be slightly puckered as the charge state of Copper is varying. Perpendicular to these CuO_2 planes are CuO_4 ribbons sharing 2 vertices. The yttrium atoms are found between the CuO_2 planes, while the barium atoms are found between the CuO_4 ribbons and the CuO_2 planes. The structure has a stacking of different layers: $(\text{CuO})(\text{BaO})(\text{CuO}_2)(\text{Y})(\text{BaO})(\text{CuO})$. In YBCO, the CuO chains are known to play an important role for superconductivity. The structure of this material depends on the oxygen content. In the chemical formula $\text{YBa}_2\text{Cu}_3\text{O}_{7-x}$ when $x = 1$, the O(1) sites in the Cu(1) layer

are vacant and the structure is tetragonal. The tetragonal form of YBCO is insulating and does not superconduct. Increasing the oxygen content slightly causes more of the O(1) sites to become occupied. For $x < .65$ CuO chains along the b axis of the crystal are formed. Elongation of the b axis changes structure to orthorhombic, with lattice parameters of $a = 3.82\text{\AA}$, $b = 3.89\text{\AA}$ and $c = 11.68\text{\AA}$.

2.2 Magnetolectric Material :

The coupling between magnetic and electric properties of a material gives rise to magneto-electric effects. The ME effects are determined by the transformation properties of the crystal in both space and time. These effects can be taken into account in the expansion of the free energy of a material, i.e:

$$F(\vec{E}, \vec{H}) = F_0 - P_i^S E_i - M_i^S H_i - \frac{1}{2} \epsilon_{ij} E_i E_j - \frac{1}{2} \mu_{ij} H_i H_j - \alpha_{ij} E_i H_j$$

where P^S and M^S denote the components of the spontaneous polarization and magnetization and ϵ_{ij} and μ_{ij} are the electric and magnetic susceptibilities respectively. The tensor α_{ij} corresponds to the induction of polarization by a magnetic fields or of magnetization by an electric field and is designated as the linear ME effect. The ME responses are limited under following relation :

$$\alpha_{ij}^2 < \epsilon_{ij} \mu_{jj} \text{ or } \alpha_{ij}^2 < \chi_{eii} \chi_{mjj}$$

From this expression it is then clear that in order to obtain the largest ME responses within one material, large dielectric constants and magnetic susceptibilities are important. Therefore, the most possible way to find ME effects is in the ferroelectrics and the ferromagnetics. The materials possessing these two properties so called multiferroics are the best candidates to show a strong ME effects. The ultimate goal is to obtain such a powerful ME effects that the electric polarization can be totally switched by magnetic field and the magnetization can be reversed by electric field as well, within a single phase. If a magnetic field is applied to such composite due to magnetostriction effect the ferromagnetic phase deforms as the electrostrictive phase is mechanically coupled with magnetostriction phase. As the electrostriction material have piezoelectric effect the spontaneous polarization of the electrostricton phase change. If an electric field is applied to the composite, the reverse effect will happen and the spontaneous magnetization changes.

2.3 BaTiO₃ - CoFe₂O₄ Magnetolectric System :

BaTiO₃ is a typical Ferroelectric materials with large Piezoelectricity. BaTiO₃ posses cubic Structure above curie temperatue i.e 120⁰C. Cubic BaTiO₃ is non ferroelectric because the center of positive and negative charge overlap as the ions are symmetrically arranged in the unit cell. Below T_c , it has tetragonal structure , in which O²⁻ ion in the BaTiO₃ crystal are shifted in the +ve c-direction. So electric dipole along the C-axis. Therefore BaTiO₃ is Ferroelectric in tetragonal structure.

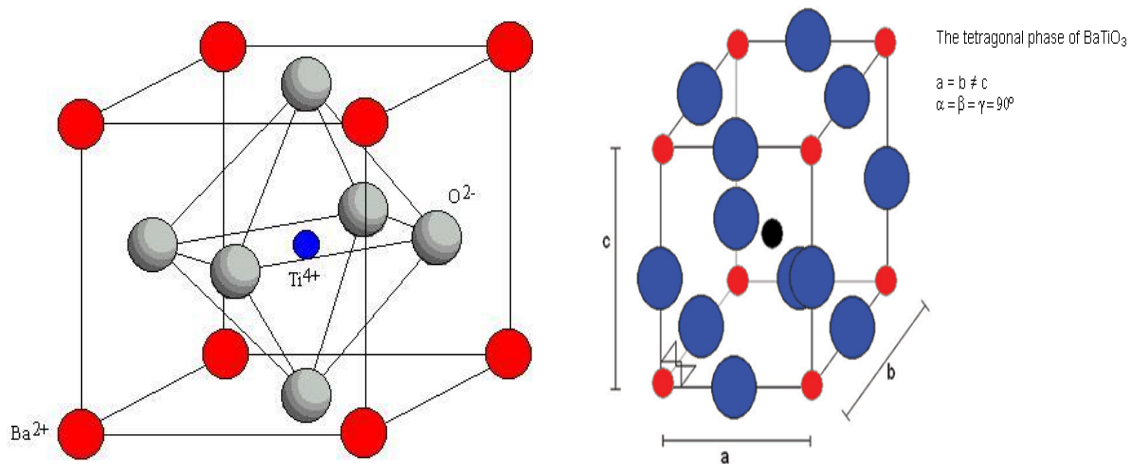


Fig.5. Unit cell of BaTiO₃ having tetragonal structure.

CoFe₂O₄ is a ferromagnetic material which belongs to the family of spinel structure. The spinel structure is named after the mineral spinel (MgAl₂O₄) and has the general composition AB₂O₄. The curie temp of CoFe₂O₄ is 500⁰C. Below T_c CoFe₂O₄ exhibit the ferromagnetic properties. It is essentially cubic, with the O- ions forming an FCC lattice.

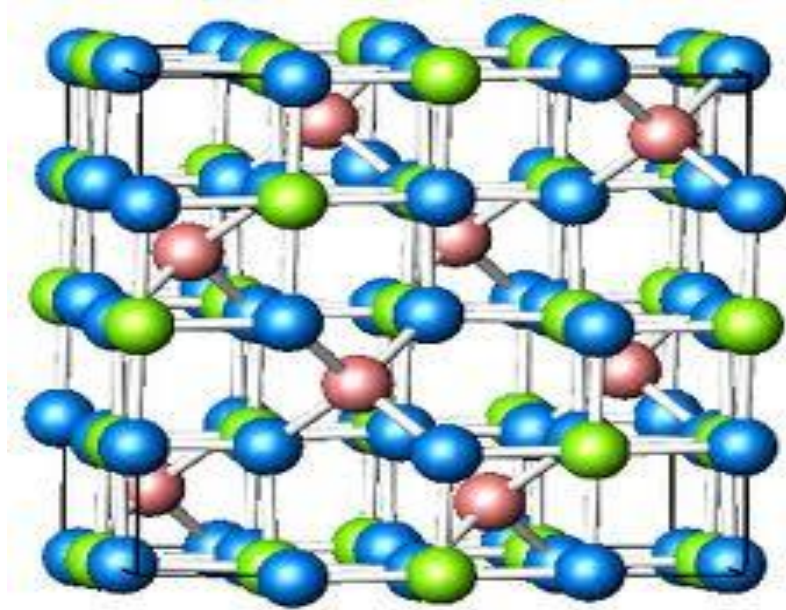


Fig.6 Crystal Structure of CoFe_2O_4

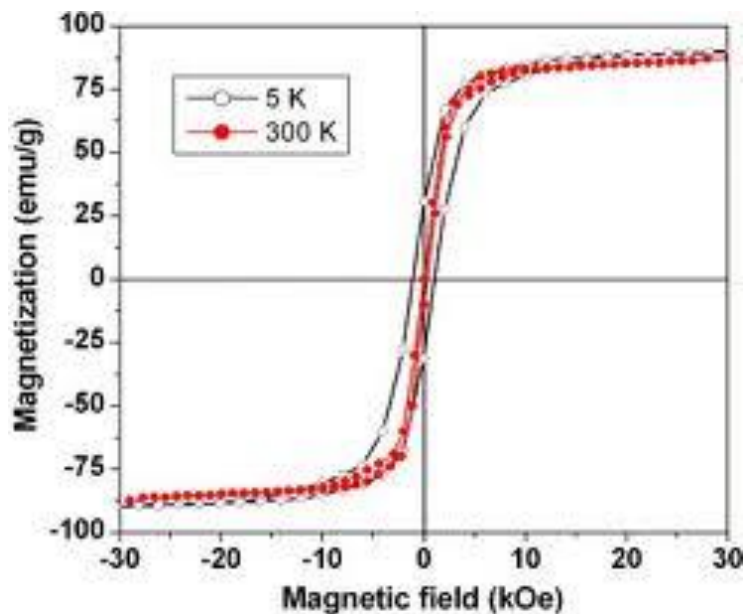


Fig.7 Magnetic hysteresis loops for CoFe_2O_4 single Crystal.

Composite of BaTiO_3 - CoFe_2O_4 combine the ferroelectricity and Ferromagnetism. The magnetoelectric coupling effect is through stress mediation .When a coupling effect is applied to the composite, there is stress generated by the CoFe_2O_4 due to its magnetostriction. Such a stress can create an electric field in the BaTiO_3 due to its piezoelectricity. The reverse process is also possible. ME materials are used as composite because of its advantageous properties. These materials are promising candidates for technological applications, since the multiferroic coupling allows the interconnection between magnetic and electric fields. New

memory devices electrically written and magnetically read have been proposed based on ME materials. BaTiO₃-CoFe₂O₄ composites are interesting magnetoelectric materials due to the individual properties of their components. CoFe₂O₄ has a spinel structure with large coercivity and magnetostriction. BaTiO₃ exhibits polymorphs depending on the temperature. The tetragonal polymorph (t-BaTiO₃) is the most interesting due to its ferroelectric and piezoelectric properties.

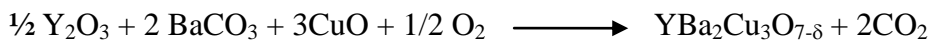
Chapter II

Experimental Procedure:

YBCO, CoFe₂O₄ and BaTiO₃ were prepared separately by solid state route method. Then composite of BaTiO₃-CoFe₂O₄ was prepared in the ratio of 70 : 30 mole %. Then they were added to YBCO in different wt.% i.e 0.0,0.2,0.4 and 0.6 respectively.

Preparation of YBCO :

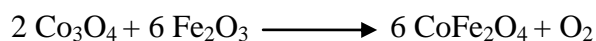
For the preparation of YBCO the precursor powders were taken as Y₂O₃, BaCO₃, CuO. It was prepared by solid state route method.



The appropriate amount of weighed chemicals were mixed in agate mortar and grind for about 2 to 3 hours till a gray powder was formed. Then heating was done at 900⁰c for about 15 hours. Repeating the calcination process 4 times with subsequent grindings assured complete removal of CO₂ by the reaction. Then the calcinide black solid were reground for 2 to 3 hours. After grinding , final pellets were made by applying pressure. Then the pellets were sintered in an alumina crucible at 920 ⁰C and annealed at 500⁰C for 8 hours in an oxygen atmosphere for oxygen uptake. Then they were slowly cooled to room temperature.

Preparation of CoFe₂O₄ :

Co₃O₄ and Fe₂O₃ have been used for the synthesis of CoFe₂O₄. In this process Co₃O₄ and Fe₂O₃ powders were mixed in 1:1 molar ratio in an agate mortar for about 3 hours with acetone as the mixing medium. Then the mixed oxides were calcined in the temperature range of 1200⁰C for 4 hours. The chemical reaction for synthesis of CoFe₂O₄ is



Preparation of BaTiO₃:

BaCO₃ and TiO₂ has been used as the precursor for the synthesis of BaTiO₃ powder by solid state route. In this process 1:1 molar ratio the precursors were mixed in an agate mortar for about 3 hrs with isopropyl alcohol as medium. The BaCO₃+TiO₂ mixed powder was calcined in temperature 1200° C for 4 hrs.

Preparation of BaTiO₃ - CoFe₂O₄ Composite:

BaTiO₃ - CoFe₂O₄ Composite Containing 70% BaTiO₃ and 30% of CoFe₂O₄ has been used for this purpose. Requisite amount of BaTiO₃ and CoFe₂O₄ powder were mixed in an agate mortar using isopropyl as mixing media. The mixing operation was carried out in a repetitive manner in order to achieve a homogeneous mixture. The dried powder was calcined at 1250° C for 4 hrs.

Chapter III

Characterization

(1) XRD Analysis :

X-ray diffraction is a versatile, non-destructive analytical method for identification and quantitative determination of various crystalline forms, known as 'phases' of compound presenting powder and thin film samples. It can also provide information on unit cell dimensions. It can also identify the fine-grained minerals such as clays and mixed layer clays that are difficult to determine optically and also measure the sample purity. X-rays have wavelengths on the order of a few angstroms, the same as typical inter-atomic distances in crystalline solids. XRD data can be analyzed to determine the proportion of the different minerals present. Other information obtained can include the degree of crystallinity of the mineral(s) present, possible deviations of the minerals from their ideal compositions, structural state of the minerals.

When a focused X-ray beam interacts with these planes of atoms, part of the beam is transmitted, part is absorbed by the sample, part is refracted and scattered, and part is diffracted. X-rays are diffracted by each mineral differently, depending on what atoms make up the crystal lattice and how these atoms are arranged. In X-ray powder diffractometry,

X-rays are generated within a sealed tube that is under vacuum. A current is applied that heats a filament within the tube, the higher the current the greater the number of electrons emitted from the filament. A high voltage, typically 15-60 kilovolts, is applied within the tube. This high voltage accelerates the electrons, which then hit a target, commonly made of copper. When these electrons hit the target, X-rays are produced. The wavelength of these X-rays is characteristic of that target. These X-rays are collimated and directed onto the sample, which has been ground to a fine powder (typically to produce particle sizes of less than 10 microns). A detector detects the X-ray signal; the signal is then processed either by microprocessor or electronically, converting the signal to a count rate. Changing the angle between the X-ray source, the sample, and the detector at a controlled rate between preset limits is an X-ray scan. When an X-ray beam hits a sample and is diffracted, we can measure the distances between the planes of the atoms that constitute the sample by applying Bragg's Law. Bragg's Law is ,

$$n \lambda = 2 d \sin \theta \text{ where}$$

n = order of the diffracted beam,

λ = wavelength of the incident X-ray beam,

d = distance between adjacent planes of atoms (the d -spacings)

θ = angle of incidence of the X-ray beam.

Since we know λ and we can measure θ , we can calculate the d -spacings. The characteristic set of d -spacing generated in a typical X-ray scan provides a unique "fingerprint" of the mineral or minerals present in the sample. When properly interpreted, by comparison with standard reference patterns and measurements, this "fingerprint" allows for identification of the materials.

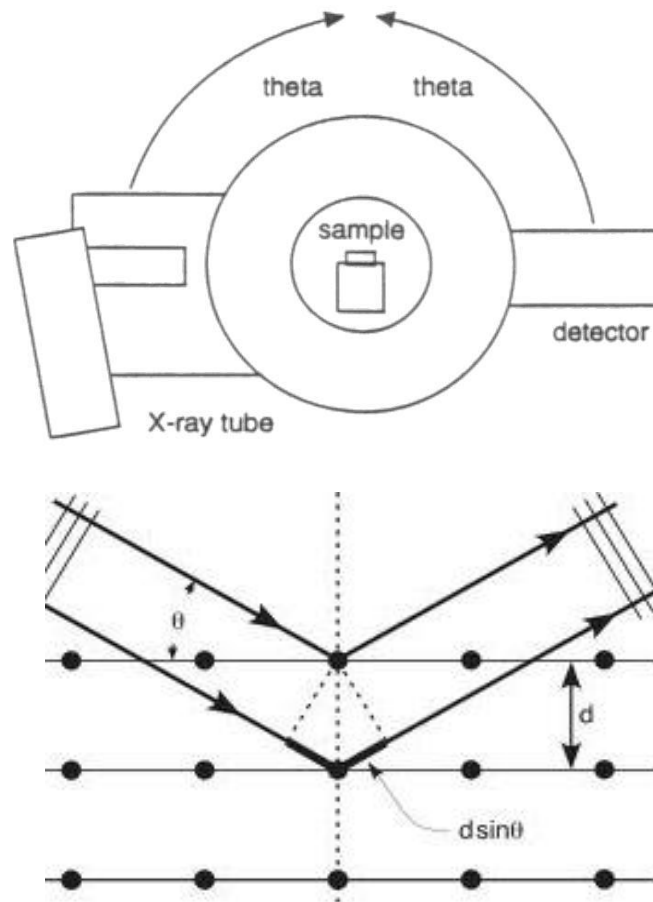


Fig.8 Simplified sketch of one possible configuration of the X-ray source (X-ray tube), the X-ray detector and the sample during an X-ray scan. In this configuration, the X-ray tube and the detector both move through θ and the sample remains stationary.

(2) R-T Measurement by Four probe method

The Four Probe Method is one of the standard and most widely used method for the measurement of resistivity. 4-point probes method is an electrical impedance measuring technique that uses separate pairs of current-carrying and voltage-sensing electrodes to make more accurate measurements than traditional two-terminal (2T) sensing. The four probes are collinear and equally spaced. The error due to contact resistance, which is specially serious in the electrical measurement, is avoided by the use of two extra contacts (probes) between the current contacts. In this arrangement the contact resistance may all be high compare to the

sample resistance, but as long as the resistance of the sample and contact resistances are small compared with the effective resistance of the voltage measuring device (potentiometer, electrometer or electronic voltmeter), the measured value will remain unaffected. Because of pressure contacts, the arrangement is also specially useful for quick measurement on different samples or sampling different parts of the same sample. The voltage drop is measured between the two probes labelled by means of a digital voltmeter. The potential drop across the contact resistance associated with probes is minimized, only the resistance associated with the superconductor between probes is measured. 4T sensing is used in some ohmmeters and impedance analyzers, and in precision wiring configurations for strain gauges and resistance thermometers. 4-point probes are also used to measure sheet resistance of thin films.

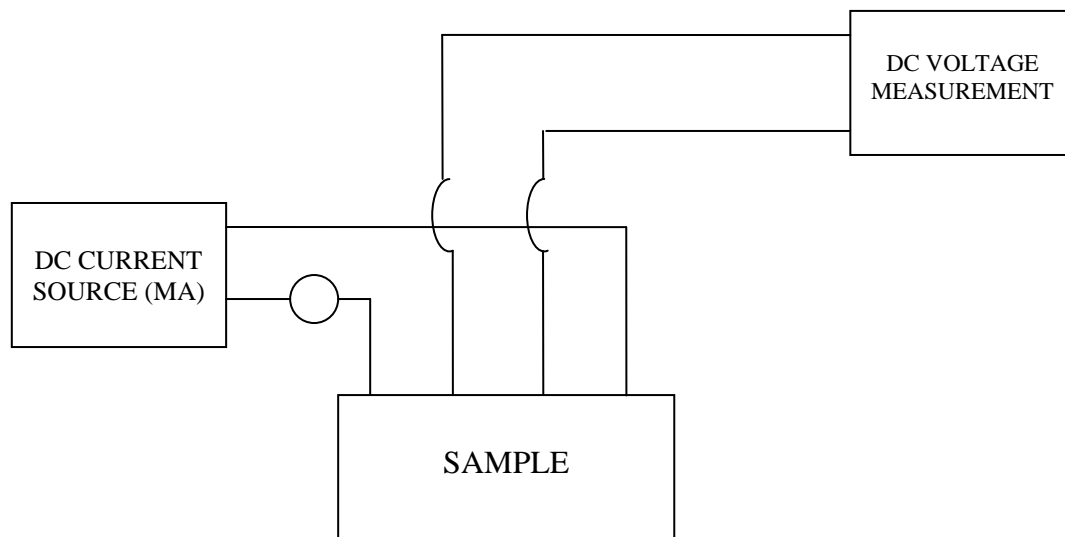


Fig.9 Four probe arrangement for resistance measurement

Chapter IV

Results and Discussion

In this section different characterization techniques have been done. Analysis of the plot with the discussion has been made.

(1) XRD Analysis :

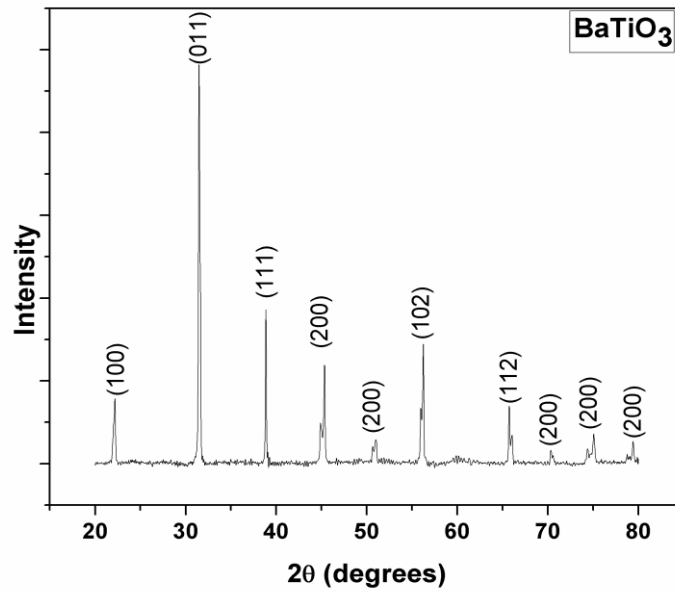


Fig.10a. XRD graphs of BaTiO₃

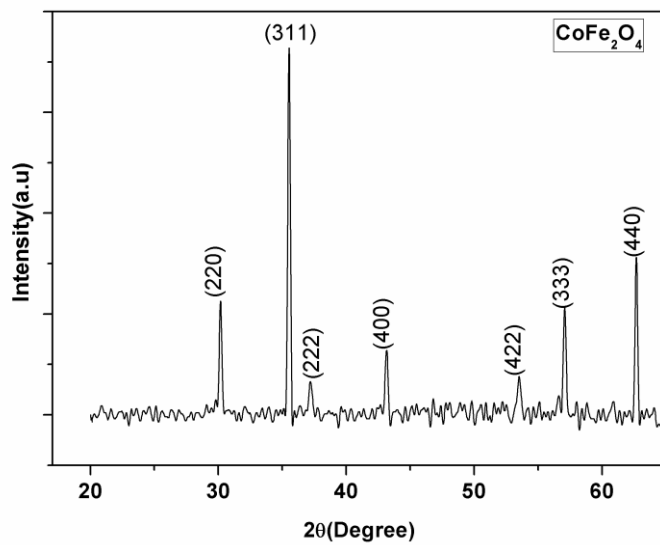


Fig.10b. XRD graphs of CoFe₂O₄

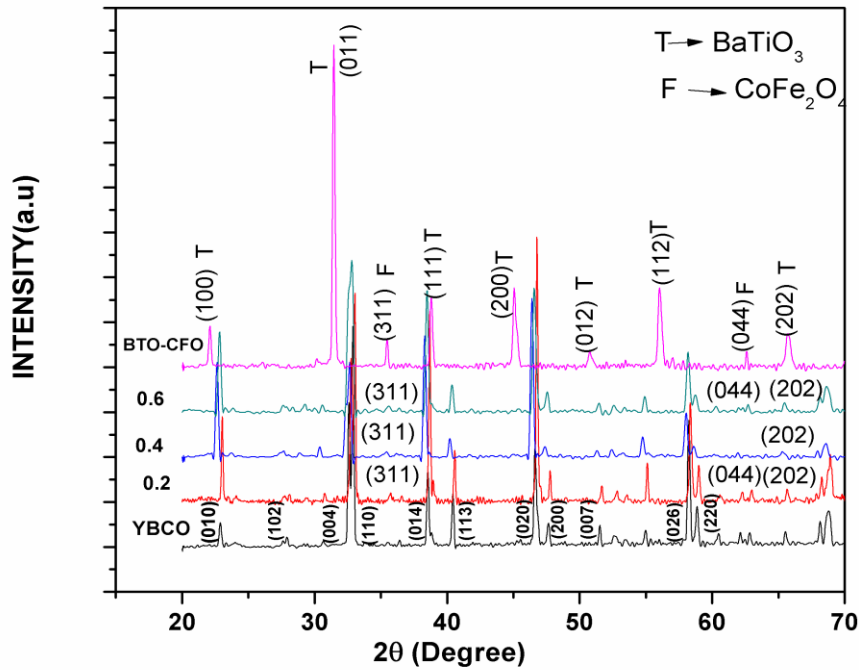


Fig.10c. XRD graphs of YBCO+ X BaTiO₃-CoFe₂O₄ (0.0,0.2,0.4,0.6) composites.

From the figure 10a and 10b the major peak (011) of BTO and (311) of CFO respectively have been identified in the composite (BTO-CFO) in figure 10c. The intensity variation of these above peaks depends on the phase formation in the composite. The diffraction pattern analysis of the composite samples of YBCO + x BTO-CFO are indexed using ChekCell software and the results are found to be in orthorhombic phase at room temperature with a space group P_{mmm} without noticeable impurity peaks. Appearance of peaks (004), (007) in the XRD pattern reveals a (00l) orientation of YBCO. The presence of CFO (311), (044) peak centered in the 2θ range of 35.51° and 62.64° respectively and BTO (202) at 65.69° gives an evidence for the formation of CoFe₂O₄ and BaTiO₃ crystallites in YBCO matrix. The intensity of (020),(113) planes increases in the composite samples, which indicates that most of the diffractions comes from these planes.

2) Resistance vs. Temperature Measurement :

Measurement of the resistivity dependence of temperature for different samples with various amounts of BTO-CFO are shown in Fig.11. All samples show metallic behaviour in the normal state ($d\rho/dT > 0$) and as superconducting transition to zero resistance.

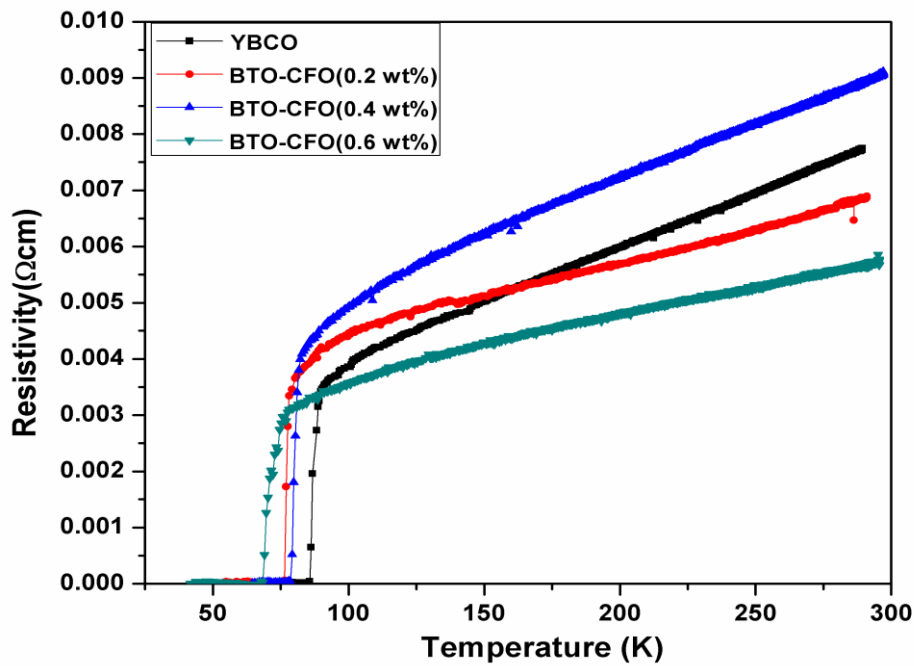


Fig.11 Temperature dependence of the resistivity for YBCO+X BaTiO₃-CoFe₂O₄ composites (X = 0.0,0.2,0.4, and 0.6 wt.%).

At higher temperature, both samples exhibited linear temperature dependence. The resistive transition exhibits two different regimes. The first is characterized by the normal state that shows a metallic behaviour (above $2T_c$). The normal resistivity is found to be linear from room temperature to a certain temperature (180 K–300 K), and in this region it follows Anderson and Zou relation given by $\rho_R(T) = a+bT$ (where a is the intercept gives the residual resistivity ρ_0 and b is the slope) and then extrapolating to T_c gives the slope. The second is the region characterized by the contribution of Cooper pairs fluctuation to the conductivity below T_c , where $\rho(T)$ is deviating from linearity. This is mainly due to the increasing rate of cooper pair formation on decreasing the temperature. Different critical temperatures are observed from the different composites. The temperature derivative of resistivity curves are

shown in fig.12. T_c is defined as the peak position of the derivative and is observed to decrease with increasing wt. % of $\text{BaTiO}_3\text{-CoFe}_2\text{O}_4$. The peak broadening is occurring due to addition of BTO-CFO composite which is affecting the intergranular weak link between grains.

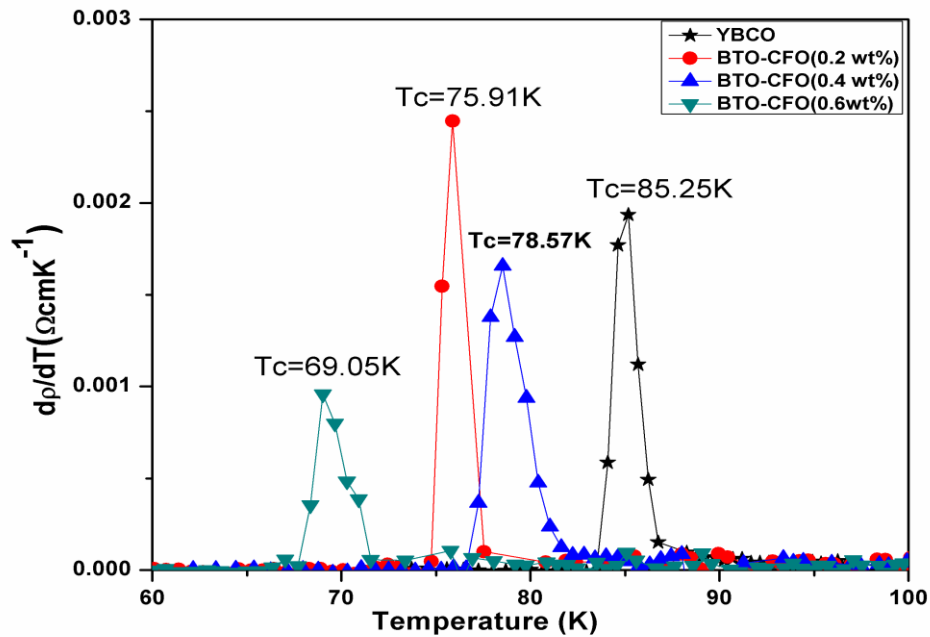


Fig.12 Temperature derivative of resistivity of YBCO + x BTO-CFO composites (x = 0.0, 0.2, 0.4, 0.6 wt. %).

Table1 Variation in T_c and T_{c0} value for YBCO+X $\text{BaTiO}_3\text{-CoFe}_2\text{O}_4$ composites.

$\text{BaTiO}_3\text{-CoFe}_2\text{O}_4$ (wt%)	T_{c0}	T_c	$\Delta T = T_c - T_{c0}$
0.0	82.99	85.20	2.21
0.2	74.19	75.94	1.75
0.4	76.62	78.55	1.93
0.6	66.39	68.99	2.60

From the above data it is clear that with increase in wt.% of BTO-CFO in YBCO the critical temperature T_c and T_{c0} decreases gradually. It is found that T_{c0} decreases and the transition width $\Delta T = T_c - T_{c0}$ decreases for 0.2 composites and again increases with increasing BTO-CFO content.

Chapter V

CONCLUSION

The effect of magnetoelectric inhomogeneity of BTO-CFO on the structural and superconducting property of YBCO is systematically studied. From R-T graph it is concluded that with increase in wt.% of BTO-CFO in YBCO matrix the critical temperature T_c and T_{c0} decreases gradually. Appearance of peaks (004), (007) in the XRD pattern reveals a (001) orientation of YBCO. The presence of CFO (311), (044) peak centered in the 2θ range of 35.51° and 62.64° respectively and BTO (202) at 65.69° gives an evidence for the formation of CoFe_2O_4 and BaTiO_3 crystallites in YBCO matrix. The intensity of (020), (113) planes increases in the composite samples, which indicates that most of the diffractions comes from these planes.

References

- [1] “Solid state physics” – S.O.Pillai
- [2] “Solid state physics”- Kittel
- [3] H.Y.Lee, S.I.Kim, Y.C.Lee, Y.P.Hong, Y.H.Park, & K.H.Ko. 13 (2003) 2743
- [4] J.F. Scott, Multiferroic memories, Nat. Mater. 6 (2007) 256–257.
- [5] J.B. Silva, W. Brito, N.D.S. Mohallem, Influence of heat treatment on cobalt ferrite ceramic powders, Mater. Sci. Eng. B 112 (2004) 182–187.
- [6] L.V. Leonel, A. Righi, W.N. Mussel , J.B. Silva , N.D.S. Mohallem , Ceramics International 37 (2011) 1259–1264
- [7] P.C. Rajath Varma, Rudra Sekhar Manna, D. Banerjee, Manoj Raama Varma, K.G. Suresh and A.K. Nigam - Journal of Alloys and Compounds - 453 (2008) 298-303
- [8] A. Mohanta, D. Behera, J. Superconductivity 23 (2010) 275.
- [9] W. Eerenstein, N. D. Mathur and J. F. Scott, Nature 442, (2006) 759.
- [10] C. N. R. Rao, Serrao, C. R. New Routes to Multiferroics. J. Mater. Chem. 17, (2007) 4931.